Synthesis of β-Lactams by Ag^+-Induced Ring Expansion of 1-Hydroxycyclopropylamines: A Theoretical Analysis

Pablo Campomanes,[†] M. Isabel Menéndez,[†] Gloria I. Cárdenas-Jirón,[‡] and Tomás L. Sordo*[,†]

Departamento de Química Física y Analítica, Facultad de Química, Universidad de Oviedo, Julián Clavería, 8, 33006 Oviedo, Principado de Asturias, Spain, and Departamento de Ciencias Químicas, Facultad de Química y Biología, Universidad de Santiago de Chile, Casilla 40, Correo 33, Santiago, Chile

Received: May 3, 2005; In Final Form: July 13, 2005

A theoretical analysis of the silver-induced ring expansion of *N*-chloro-*N*-methyl-1-hydroxycyclopropylamine to form *N*-methyl-2-azetidinone, and of the Cl^- elimination from this substrate without Ag^+ assistance, was performed using the B3LYP method and the 6-31+G(d) basis set for C, N, O, H, and Cl atoms and the relativistic effective core pseudopotential LANL2DZ complemented with one set of f polarization functions ($\zeta_f = 0.473$) for the Ag atom. The partial Ag^+-assisted extrusion of Cl^- at the rate-determining transition state provokes an important change in the nodal properties of the frontier molecular orbitals of the $H_3CClNCOHAg^+$ fragment, thus making very stabilizing HOMO−LUMO interactions between this fragment and the C_2H_4 moiety possible. This interaction leads to the ring opening and release of most of the strain energy, giving rise to a low energy barrier for the process. Also, by assisting the Cl^- extrusion, Ag^+ avoids the elimination of the hydroxyl hydrogen atom, which would provoke the fragmentation of the system instead of the formation of the β-lactam.

Introduction

The synthesis of β-lactams has received considerable attention in the past few years because of their potential antibacterial activity[1−7] and their role as precursors in the preparation of different natural and unnatural products.[8,9] Among the many synthetic methods developed to obtain β-lactams (the Staudinger cycloaddition reaction between ketenes and imines, the ester enolate-imine condensation, the cyclization of β-amino carboxylic acids and esters, the cyclizations of β-functionalized amides, imidates, and hydroxamates, the cycloaddition of chromium-carbene complexes with imines, the oxidation of azetidines, and the ring contraction of 4-azido-2-pyrrolinones to 3-cyano-2-azetidinones),[1−7] one of the most appealing routes is the ring enlargement of amine adducts across cyclopropanones, initially proposed by Wasserman et al.[10−15] This author has presented a general application of this method (see Scheme 1) that consists of adding primary amines to cyclopropanone **A** to get labile carbinolamine **B**, which may be converted to *N*-chloro derivative **C** by addition of *tert*-butyl hypochlorite (Gassman reaction). Treatment of the *N*-halo derivative with silver ion in acetonitrile leads to the formation of β-lactam **D**.[11] This method has been extended for the preparation of β-lactams from amino acid esters,[14] which participate in the sequence shown in Scheme 1 in the place of the primary amine. The major drawback of this elegant synthesis is the difficult accessibility of cyclopropanone, but in the last years this procedure has reappeared in the literature as a regioespecific rearrangement to obtain 1,4,4-trisubstituted 2-azetidinones from conveniently substituted cyclopropanones.[16]

In a previous investigation, we studied the silver-induced ring expansion of *N*-chloro-*N*-methyl-2,2-dimethyl-1-hydroxycyclopropylamine and *N*-chloro-*N*-methyl-1-hydroxy-2-methoxycarbonyl-2-methylcyclopropylamine to yield the corresponding 4,4-disubstituted-2-azetidinones.[17] In that work we found that both processes are regioespecific and proceed very easily in dichloromethane through Gibbs energy barriers of 1.2 and 4.3 kcal mol^{-1}, respectively. However, the origin of the readiness of those two ring-expansion reactions and the role played by the silver cation in their mechanism are two important issues that need further investigation. A more efficient use of any synthetic tool requires a deeper understanding of the mechanism of the process. This deeper insight can be gained by extracting the wealth of information contained in the orbitals and electron density of the system. To this end, here we present a theoretical analysis of the silver-induced ring enlargement of *N*-chloro-*N*-methyl-1-hydroxycyclopropylamine to form *N*-methyl-2-azetidinone, and of the Cl^- elimination from this substrate without Ag^+ assistance.

SCHEME 1: Preparation of 2-Azetidinones from Cyclopropanone

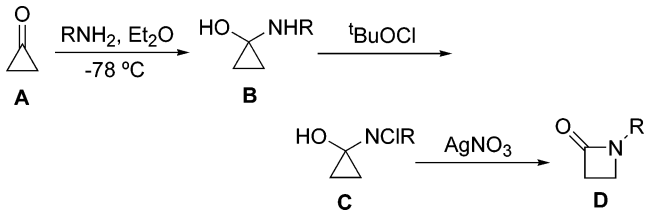

Computational Details

Quantum chemical computations were performed using the Gaussian 98 series of programs[18] with the hybrid density functional B3LYP method,[19] which combines Becke's three parameter nonlocal hybrid exchange potential with the nonlocal correlation functional of Lee, Yang, and Parr. The 6-31+G(d)

* Corresponding author. E-mail: tsordo@uniovi.es.
[†] Universidad de Oviedo.
[‡] Universidad de Santiago de Chile.

10.1021/jp052291+ CCC: $30.25 © 2005 American Chemical Society
Published on Web 08/09/2005

basis set[20] for C, N, O, H, and Cl atoms, and the relativistic effective core pseudopotential LANL2DZ[21] complemented with one set of f polarization functions ($\zeta_f = 0.473$) for Ag were used in the calculation. The geometries of stable species were fully optimized using Schlegel's algorithm.[22] Harmonic vibrational frequencies were calculated at this same theory level to characterize the critical points located and to evaluate the zero-point vibrational energy (ZPVE). Intrinsic reaction coordinate (IRC) calculations were also carried out to check the connection between the TSs and the minimum energy structures using the Gonzalez and Schlegel method[23] implemented in Gaussian 98.

Thermodynamic data, ΔH, ΔS, and ΔG (298.15 K, 1 atm), were computed using the B3LYP frequencies within the ideal gas, rigid rotor, and harmonic oscillator approximations.[24]

To take into account condensed-phase effects, we used a self-consistent-reaction-field (SCRF) model proposed for quantum chemical computations on solvated molecules.[25−27] The solvent is represented by a dielectric continuum characterized by its relative static dielectric permittivity, ϵ. The solute, which is placed in a cavity created in the continuum after spending some cavitation energy, polarizes the continuum, which in turn creates an electric field inside the cavity. This interaction can be taken into account using quantum chemical methods by minimizing the electronic energy of the solute plus the Gibbs energy change corresponding to the solvation process that is given by[28]

$$\Delta G_{\text{solvation}} = -\frac{1}{2} E_{\text{int}}$$

where E_{int} is the solute−solvent electrostatic interaction energy

$$E_{\text{int}} = \sum_{\alpha} V_{\text{el}}(R_\alpha) Z_\alpha - \int V_{\text{el}}(r)\rho(r)\, \mathrm{d}r$$

In this equation, V_{el} is the electrostatic potential created by the polarized continuum in the cavity, R_α and Z_α are the position vector and charge of the nucleus α, respectively, and $\rho(r)$ is the electronic charge density at point r. We calculated the electrostatic potential, V_{el}, by employing the united atom Hartree−Fock (UAHF) parametrization of the PCM[26,29] model as implemented in Gaussian 98. The solvation Gibbs energies, $\Delta G_{\text{solvation}}$, along the reaction coordinate were evaluated from single-point PCM-UAHF calculations on the gas-phase optimized geometries at the B3LYP/6-31+G(d)-LANL2DZ level. Relative permittivities of 8.93 and 36.6 were assumed in the calculation to simulate CH_2Cl_2 and CH_3CN as the solvents used in experimental work.

The B3LYP electron densities were analyzed by means of the theory of atoms in molecules developed by Bader[30] using the AIMPAC package of programs.[31] The Kohn−Sham determinants of the most important critical structures located along the reaction coordinate were also studied by means of a theoretical method developed by Fukui's group.[32] This method is based on the expansion of the molecular orbitals (MOs) of a complex system, AB, in terms of the MOs of its constituent fragments, A and B, using the geometry each fragment has in the corresponding critical structure and the performance of the configurational analysis. The configurational analysis is performed by writing the determinant constructed by the Kohn−Sham MOs of the complex system, Ψ, by a combination of various fragment electronic configurations

$$\Psi = C_0\Psi_0 + \sum C_q\Psi_q$$

where Ψ_0 (zero configuration, AB) is the state in which neither electron transfer nor electron excitation takes place and Ψ_q stands for monotransferred configurations, $\Psi_{o\rightarrow u'}$, in which one electron in an occupied MO, o, in one of the two fragments A or B is transferred to an unoccupied MO, u′, of the other fragment (A^+B^-, and A^-B^+ configurations), monoexcited configurations, $\Psi_{o\rightarrow u}$, in which one electron in an occupied MO, o, of any of the two fragments is excited to an unoccupied MO, u, of the same fragment (A*B and AB* configurations), and so on. This configuration analysis, which has proved useful for understanding the physicochemical features of chemical interactions, was performed by means of the ANACAL program.[33] The Kohn−Sham orbitals were also analyzed by means of an NBO (Natural Bond Orbital) analysis.[34]

Results and Discussion

First we present the results obtained for the ring expansion of *N*-chloro-*N*-methyl-1-hydroxycyclopropylamine assisted by Ag^+, eq 1, and then the mechanism found for the elimination of HCl from this same substrate in the absence of Ag^+.

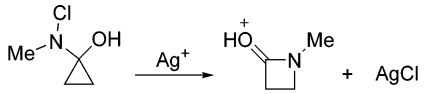

(1)

Ring Expansion of *N*-Chloro-*N*-methyl-1-hydroxycyclopropylamine in the Presence of Ag^+. *N*-Chloro-*N*-methyl-1-hydroxycyclopropylamine can exist in two isomeric forms with the hydrogen atom bonded to the oxygen in the syn or anti position with respect to Cl, respectively (see Figure 1). The syn isomer in Gibbs energy in CH_2Cl_2 (CH_3CN) solution is 0.6 (0.2) kcal mol^{-1} more stable than the anti one (see Table 1), with both conformers being connected through a transition state (TS) 3.6 kcal mol^{-1} above the syn isomer in both solvents. Despite this, the anti isomer presents the most adequate conformation to interact with Ag^+ along the reaction coordinate for reaction 1 and thus we will consider the process for this isomer.

We will report first the electronic energy profile including the zero-point vibrational energy (ZPVE) correction and then the Gibbs energy profile both in the gas-phase and in solution.

Reaction 1 proceeds under the energy level corresponding to the reactants and starts with the formation of an adduct, **CAG**, 39.8 kcal mol^{-1} more stable than the reactants, in which Ag^+ bonds simultaneously to the chlorine atom at a distance of 2.656 Å and to the oxygen atom at a distance of 2.384 Å. The cyclopropyl ring remains at **CAG** practically unaltered. **CAG** can evolve to the nitrenium intermediate, **I**, and a AgCl molecule, 37.0 kcal mol^{-1} under reactants, through **TSCAGI**, 4.6 kcal mol^{-1} above **CAG**. At **TSCAGI**, AgCl is practically formed as the AgCl bond distance is 2.453 Å (at the theory level employed by us the bond distance in the isolated AgCl is 2.362 Å). Both C1−C2 and C1−C3 bonds lengthen, particularly C1−C3 that becomes 1.650 Å (see Figure 1 for atom numbering). **I** evolves through the TS **TSIP** for rotation about the C1−C2 bond and formation of the new C3−N bond with an energy barrier of 0.4 kcal mol^{-1} to yield the final protonated β-lactam + AgCl, 84.9 kcal mol^{-1} more stable than separate reactants.

In the gas phase, the thermal correction to the energy is similar for all of the critical structures along the reaction coordinate. Entropy destabilizes **CAG** and **TSCAGI** by about 7−8 kcal mol^{-1}, whereas it favors the remaining structures with respect to reactants by 4 kcal mol^{-1}, approximately. As a consequence, in Gibbs energy in the gas phase the barrier corresponding to **TSCAGI** is 3.8 kcal mol^{-1} and the exothermicity of the process is 88.5 kcal mol^{-1}.

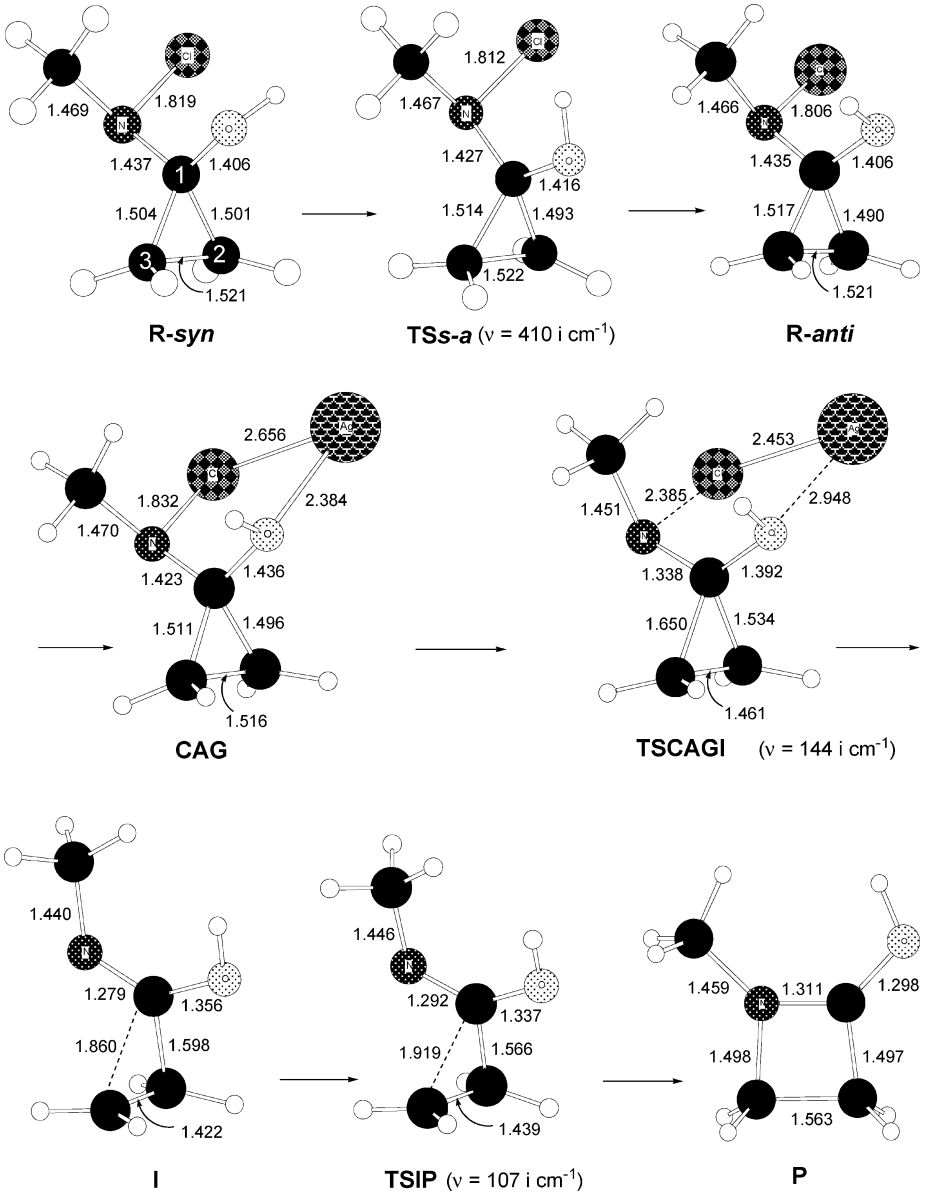

Figure 1. B3LYP optimized geometries corresponding to the critical structures located along the Ag^+-assisted ring expansion of *N*-chloro-*N*-methyl-1-hydroxycyclopropylamine.

TABLE 1: Relative B3LYP Electronic Energies Including the ZPVE Correction, Enthalpies, Solvation Energies, and Gibbs Energies in the Gas Phase and in Solution (kcal mol^{-1}) for the Critical Structures Located along the Reaction Coordinate for the Ag^+-Assisted Ring Expansion of *N*-Chloro-*N*-methyl-1-hydroxycyclopropylamine

structure	$\Delta(E_{elec} + ZPVE)$	ΔH	ΔG_{gas}	$\Delta\Delta G_{solvation}$ CH_2Cl_2/CH_3CN	$\Delta G_{solution}$ CH_2Cl_2/CH_3CN
R-syn + Ag^+	−2.5	−2.5	−2.5	1.8/2.3	−0.6/−0.2
TSs-a + Ag^+	1.8	1.5	1.9	1.2/1.5	3.0/3.4
R-anti + Ag^+	0.0	0.0	0.0	0.0/0.0	0.0/0.0
CAG	−39.8	−40.0	−32.1	28.2/31.1	−3.9/−1.0
TSCAGI	−35.2	−35.3	−28.3	27.5/29.6	−0.8/1.3
I + AgCl	−37.0	−36.4	−41.2	17.5/19.6	−23.7/−21.6
TSIP + AgCl	−36.6	−36.7	−40.1	17.1/19.1	−23.0/−21.0
P + AgCl	−84.9	−84.9	−88.5	16.7/18.7	−71.8/−69.8

Owing to the point charge of Ag^+, CH_2Cl_2 (CH_3CN) solvent effects stabilize separate reactants considerably by about 28 (31) kcal mol^{-1} with respect to **CAG** and **TSCAGI**, and about 17 (19) kcal mol^{-1} with respect to the rest of the energy profile. Thus, in solution, the adduct **CAG** and the intermediate **I** + AgCl are 3.9 (1.0) and 23.7 (21.6) kcal mol^{-1} more stable than the initial reactants. The Gibbs energy barriers corresponding to **TSCAGI** and **TSIP** 3.1 (2.3) and 0.7 (0.6) kcal mol^{-1}, respectively, and the exothermicity of the process is 71.8 (69.8) kcal mol^{-1}. We see then that the solvent with larger relative permittivity (CH_3CN) renders a lower energy barrier for the rate-determining step of this process. The Gibbs energy profile in solution for this reaction is displayed in Figure 2.

Let us now analyze the critical structures located in the first stage of the process, which is the rate-determining one, to elucidate the assistance role played by Ag^+. It is well-known that ring strain can make three-member ring compounds particularly reactive. However, we have found when studying

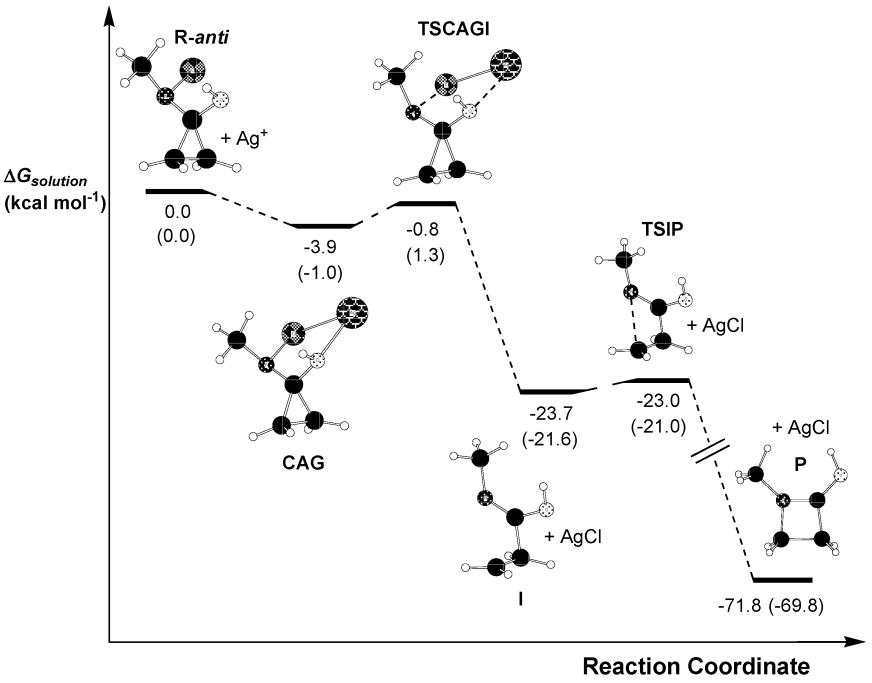

Figure 2. Gibbs energy profiles in CH_2Cl_2 (CH_3CN) solution for the Ag^+-assisted ring expansion of *N*-chloro-*N*-methyl-1-hydroxycyclopropylamine.

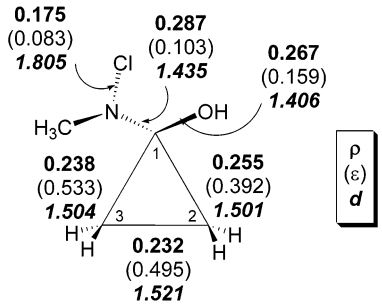

Figure 3. Most important bond lengths (Å) of *N*-chloro-*N*-methyl-1-hydroxycyclopropylamine, and the corresponding electron density, ρ, (au) and ellipticity, ϵ, evaluated at the bond critical points.

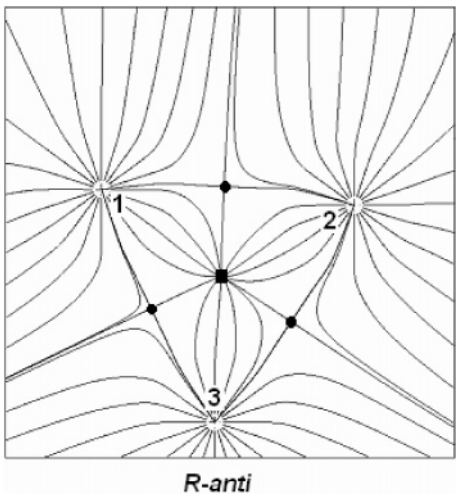

Figure 4. Map of the gradient vector field of the electronic charge density of *N*-chloro-*N*-methyl-1-hydroxycyclopropylamine in the plane containing the nuclei of the ring. Bond critical points are denoted by solid circles and the ring critical point by a solid square.

the ammonolysis of 2-azetidinone that although the release of the strain energy (28.9 kcal mol^{-1}) is the main thermodynamic factor favoring the process, its kinetic influence is quite moderate because it takes place after the transition state.[35] So an issue of interest in the present study is whether the strain energy of *N*-chloro-*N*-methyl-1-hydroxycyclopropylamine will contribute to facilitate the ring opening of the molecule and consequently the whole process or not. The importance of the strain energy accumulated would explain the exothermicity of the formation of the nitrenium intermediate, but will this strain energy facilitate the opening of the ring?

A topological analysis of the electron density of *N*-chloro-*N*-methyl-1-hydroxycyclopropylamine (see Figures 3 and 4) shows the existence of a C1−C2−C3 ring critical point (ρ = 0.197 au) and clearly reflects the presence of an important strain in this ring through the outwardly curved bond paths that determine an important ellipticity for the three constituent C−C bonds. These bonds have ellipticity values similar to those found for cyclopropane (ϵ = 0.49),[30] whose strain energy is 27.5 kcal mol^{-1}.[36] The differences between the geometric and the bond path angles of the ring are about 15−18° (see Table 2) also similar to the value reported for cyclopropane (18.8°).[30]

The configurational analysis of the electronic structure of *N*-chloro-*N*-methyl-1-hydroxycyclopropylamine in terms of the fragments A = C_2H_4 and B = CH_3ClN-C-OH (see Table 3)

TABLE 2: Differences between the Geometric Angles, α_c, and the Bond Path Angles, α_b, Found for the Three-Member Ring of *N*-Chloro-*N*-methyl-1-hydroxycyclopropylamine

angle	α_c (deg)	α_b (deg)	$\Delta\alpha = \alpha_b - \alpha_c$ (deg)
1	60.8	79.0	18.2
2	60.5	76.8	16.3
3	58.8	74.4	15.6

shows that the coefficients of the zero configuration and all of the monotransfers and monoexcitations are null. These data clearly indicate that HOMO−LUMO interactions between fragments A and B lead to no stable species and bonding has to be formed by pseudoexcitation.[37] In effect, from Figure 5 we see that in *N*-chloro-*N*-methyl-1-hydroxycyclopropylamine the HOMO−LUMO interactions between the constituent fragments considered are symmetry forbidden, HOMO−HOMO and LUMO−LUMO interactions being responsible for the molecular cohesion.

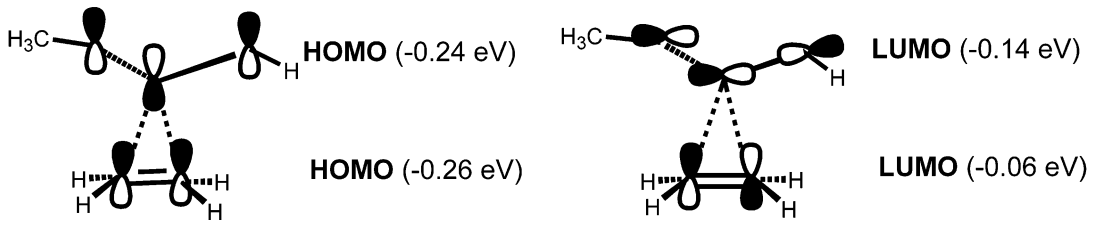

Figure 5. HOMO−HOMO and LUMO−LUMO interactions in *N*-chloro-*N*-methyl-1-hydroxycyclopropylamine (A = C_2H_4; B = CH_3ClN-C-OH).

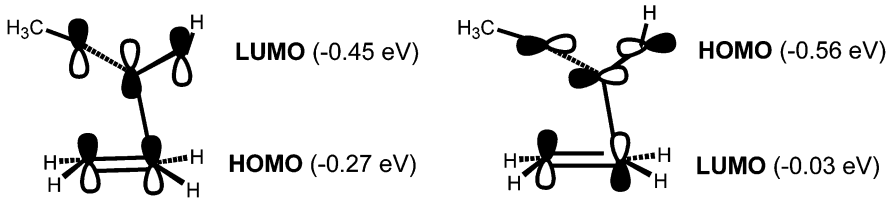

Figure 6. HOMO−LUMO interactions in the nitrenium intermediate (A = C_2H_4; B = CH_3N-C-OH^+)

TABLE 3: Coefficients and Relative Weights of the Most Important Electronic Configurations for *N*-Chloro-*N*-methyl-1-hydroxycyclopropylamine (A = C_2H_4; B = CH_3ClN-C-OH)

configuration	relative weight/coefficient
A*B* (HO−LU/HO−LU)	1.0/0.47
A^+B^{*-} (HO−LU/HO−LU)	0.57/−0.35
A^-B^{*+} (HO−LU/HO−LU)	0.41/0.30
$A^{*+}B^-$ (HO−LU/HO−LU)	0.41/0.30
$A^{*-}B^+$ (HO−LU/HO−LU)	0.33/−0.27

TABLE 4: Coefficients and Relative Weights of the Most Important Electronic Configurations for the Nitrenium Intermediate (A = C_2H_4; B = CH_3N-C-OH^+)

configuration	relative weight/coefficient
A^+B^- (HO−LU)	1.0/0.72
AB	0.65/0.58
$A^{2+}B^{2-}$ (HO−LU/HO−LU)	0.29/0.39

At the intermediate, **I**, the C1−C2 bond is still appreciably bent (ϵ = 0.450) but the ellipticity of the C2−C3 bond has considerably diminished (ϵ = 0.120) and neither a bond critical point for C1−C3 nor a ring critical point were found. Therefore, at this point of the reaction coordinate the three-member ring is open and most of the strain energy has already been emitted.

The configurational analysis of this intermediate in terms of the fragments A = C_2H_4 and B = CH_3N-C-OH^+ shows that the electronic structure of this species is determined by the HOMO−LUMO transfer from the C_2H_4 moiety and the zero configuration, with no pseudoexcitation being present already (see Table 4). As can be seen from the nodal properties of the frontier orbitals of A and B in Figure 6, the ordinary HOMO−LUMO interactions between the constituent fragments are now symmetry allowed.

Therefore, we see that the system has undergone a deep electronic restructuring from separate reactants through the intermediate at the end of the first stage of the process. How has this evolution taken place?

The situation for the adduct formed between *N*-chloro-*N*-methyl-1-hydroxycyclopropylamine and Ag^+, **CAG**, is completely analogous to that in the reactant. The ring remains practically undistorted with ellipticity values very similar to those for the reactant, and no strain energy has been released, whereas the ethylenic moiety is still connected to the rest of the system through pseudoexcitation because the HOMO−LUMO overlap between the constituent fragments is null.

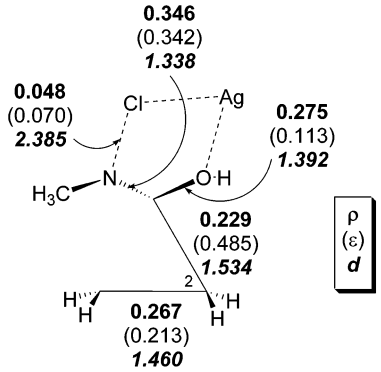

Figure 7. Most important bond lengths (Å) of the TS for AgCl elimination, **TSCAGI**, and the corresponding electron density, ρ, (au) and ellipticity, ϵ, evaluated at the bond critical points.

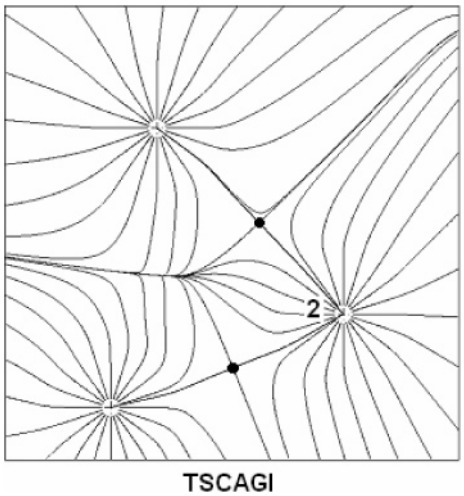

Figure 8. Map of the gradient vector field of the electronic charge density of the TS for AgCl elimination, **TSCAGI**, in the plane containing the C1, C2, and C3 nuclei. Bond critical points are denoted by solid circles.

A topological analysis of the electron density shows that in the TS for the elimination of AgCl, **TSCAGI**, there is neither a bond critical point between C1 and C3 nor a C1−C2−C3 ring critical point, and that the ellipticity value for C2−C3 has diminished to half of the original value in the reactant (see Figures 7 and 8). Therefore, at this point of the reaction coordinate most of the strain energy has been released, contributing to the stabilization of this structure. The ellipticity

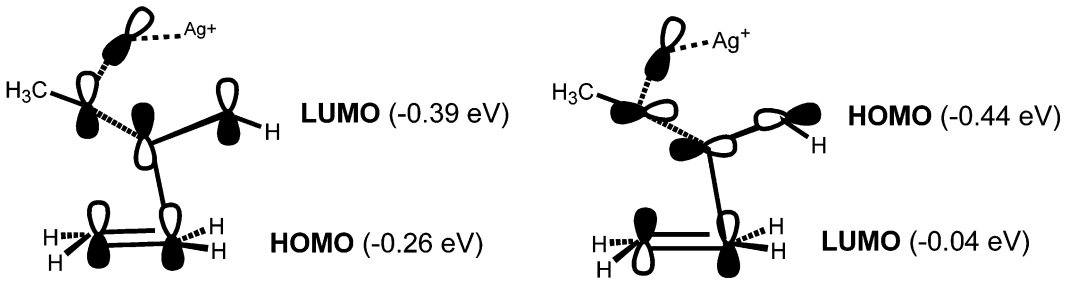

Figure 9. HOMO−LUMO interactions in the TS for AgCl elimination, **TSCAGI**, (A = C_2H_4; B = $CH_3ClNCOHAg^+$).

TABLE 5: Coefficients and Relative Weights of the Most Important Electronic Configurations for the TS for AgCl Elimination, TSCAGI, (A = C_2H_4; B = $CH_3ClNCOHAg^+$)

configuration	relative weight/coefficient
A^+B^- (HO−LU)	1.0/−0.32
$A^{2+}B^{2-}$ (HO−LU/HO−LU)	0.88/0.30
$A^{\pm}B^{\mp}$ (HO−LU/HO−LU)	0.66/0.26
A^+B^{*-}(HO−LU/HO−LU)	0.61/0.25

for C1−N indicates the formation of a double bond between these two atoms.

A configurational analysis of this TS in terms of the fragments A = C_2H_4; B = $CH_3ClNCOHAg^+$ reveals that its electronic structure is determined by the electron transfer from the HOMO-(A) to the LUMO(B) and by an important back-donation from the HOMO(B) to the LUMO(A) (see Table 5).

These data reveal an important change in the electronic structure of the system. The partial extrusion of Cl^- assisted by Ag^+ affects drastically the frontier orbitals of the fragment ($CH_3ClNCOHAg^+$), provoking an inversion of their nodal properties as displayed in Figure 9. Consequently, from this point of the reaction coordinate the HOMO−LUMO interactions between the constituent fragments are possible. Further, these HOMO−LUMO interactions are very stabilizing owing to the important stabilization of the frontier molecular orbitals of the $CH_3ClNCOHAg^+$ fragment by the positive charge supplied by the assisting Ag^+ ($\epsilon_{HOMO} = -0.44$ eV, $\epsilon_{LUMO} = -0.39$ eV, to compare with the corresponding values for the reactant in Figure 5).

An NBO analysis of this TS yields as the most important Lewis structure that with an electron lone pair at C1 and a two-electron three-enter (C1−C2−C3) interaction (I in Figure 10). This analysis also renders a second important Lewis structure generated by a C1 lone pair donor → C1−C2−C3 three-center antibonding acceptor orbital interaction (II in Figure 10). We see that the HOMO(A)−LUMO(B) interaction is now reflected in the first Lewis structure through the three-center interaction, whereas the second Lewis structure reflects the HOMO(B)−LUMO(A) interaction. Further, these two structures show that the net effect of these HOMO−LUMO interactions is the opening of the three-member cycle by cleavage of the C1−C3 bond and the release of the strain energy in agreement with the Bader analysis above.

Because of the release of the strain energy and the very efficient HOMO−LUMO interactions at this point of the reaction coordinate, the energy barrier corresponding to this TS for AgCl extrusion is low and the system can readily evolve through it to form the nitrenium intermediate.

Elimination of Chloride from *N*-Chloro-*N*-methyl-1-hydroxycyclopropylamine without Ag^+ Assistance. Trying to get a deeper insight into the role played by Ag^+ in the above process, we studied the mechanism of Cl^- elimination from *N*-chloro-*N*-methyl-1-hydroxycyclopropylamine in the absence of Ag^+.

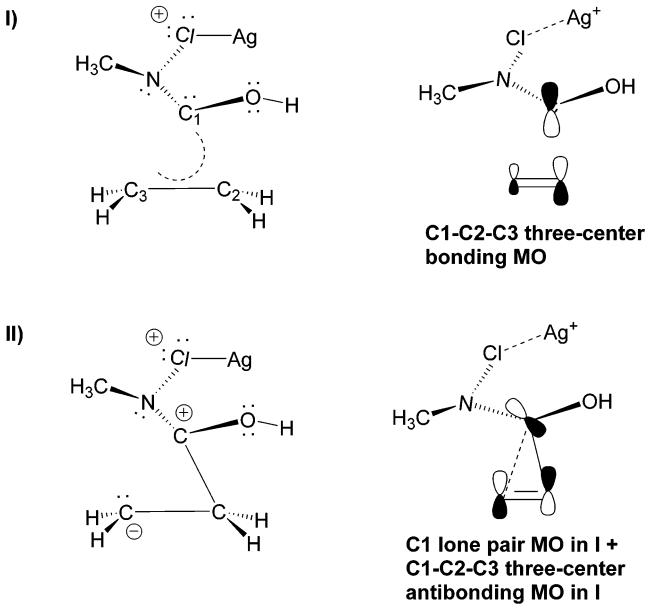

Figure 10. Most important Lewis structures for the TS for the elimination of a AgCl molecule, **TSCAGI**.

We will report first the electronic energy profile including the ZPVE correction and then the Gibbs energy profile both in the gas-phase and in solution.

This process takes place from the syn isomer through a TS, **TSRCP**, with an energy barrier in electronic energy + ZPVE of 20.2 kcal mol^{-1} to give a product complex, **CP**, with an energy of −38.8 kcal mol^{-1}, in which HCl, ethylene, and *N*-methylisocianate are interacting in a circular arrangement. In **TSRCP**, the two ring C−C bonds in which the substituted carbon atom is involved are stretched to approximately the same value of 1.627 Å (see Figure 11), and the leaving Cl^- (2.813 Å away from the nitrogen atom) is interacting with the hydroxyl hydrogen atom at a distance of 2.143 Å. This interaction is favored by the adequate orientation of the H atom in the syn isomer. No TS was located for the Cl^- elimination from the anti isomer, which would evolve then through transformation into the syn isomer to undergo this process. Finally, the complex **CP** dissociates to yield HCl + ethylene + *N*-methylisocianate 3.2 kcal mol^{-1} above it. Thus, when the elimination of Cl^- is not assisted by Ag^+ the system decomposes into ethylene, HCl, and *N*-methylisocianate instead of yielding a β-lactam.

The thermal correction to the energy of **TSRCP** is practically the same as that of the initial reactant, but **CP** and the final products become destabilized in ΔH by about 3 kcal mol^{-1}. Entropy slightly stabilizes **TSRCP** by 0.3 kcal mol^{-1}, whereas **CP** and the products are appreciably favored by it by about 13 and 25 kcal mol^{-1}, respectively.

The effect of solvent lowers the energy barrier for the process and increases its exothermicity, producing the $\Delta G_{solution}$ profile

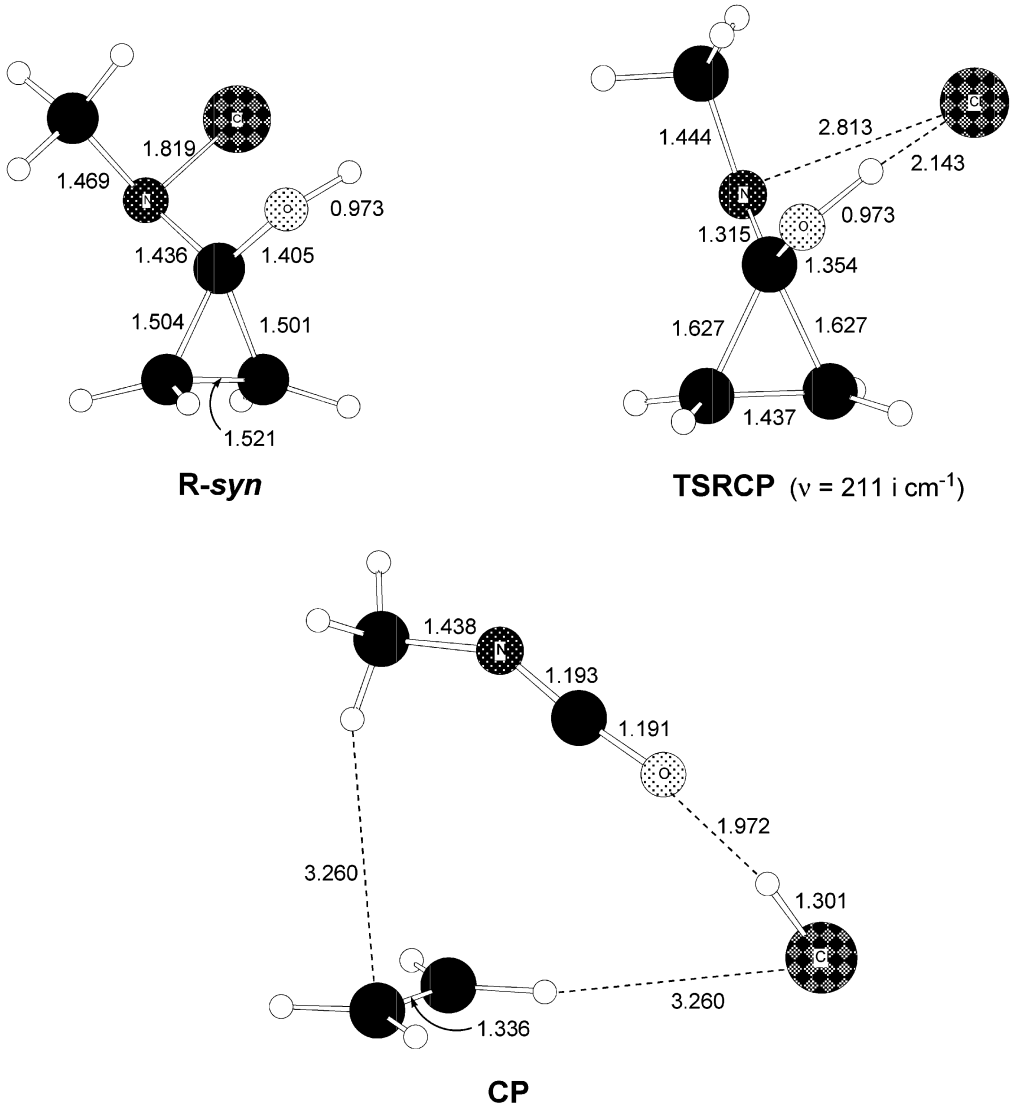

Figure 11. B3LYP optimized geometries corresponding to the critical structures located along the reaction coordinate for the elimination of HCl from *N*-chloro-*N*-methyl-1-hydroxycyclopropylamine without Ag^+ assistance.

presented in Figure 12. In CH_2Cl_2 (CH_3CN) solution, the product complex, **CP**, becomes a transient structure and the reaction concerted with a Gibbs energy barrier of 10.4 (8.8) kcal mol^{-1} and an exothermicity of 62.2 (60.7) kcal mol^{-1}. We see then that the larger the permittivity of the solvent the lower the energy barrier for this process.

Let us now analyze the TS for the elimination of Cl^-, **TSRCP**. A topological analysis of the electron density shows (see Figures 13 and 14) that in **TSRCP** the original ring remains closed with an electron density at the ring critical point of 0.176 au, lower than in the reactant. Therefore, in this case the cannot contribute to the stabilization of the TS reducing its corresponding energy barrier. It is interesting that, as we can see in the molecular graph in Figure 14, the bond paths corresponding to C1−C2 and C1−C3 are curved inwardly, determining important ellipticity values for these bonds[30] and a negative value for the difference between the geometric and bond path angle 1 (see Table 7). The two bonds, C1−C2 and C1−C3, have weakened appreciably, diminishing their bond critical electron density. As indicated above, the ring critical electron density has also undergone a parallel reduction while these two bond critical points get closer to it tending to coalescence. All of these facts clearly show that this ring is unstable with respect to its fragmentation by extrusion of an ethylenic moiety.

A configurational analysis of this TS in terms of the fragments A = C_2H_4; B = $CH_3ClN-C-OH$ shows (see Table 8) that now the most important electronic configurations of **TSRCP** are the electron transfer from the ethylene moiety, the zero configuration, and the back-donation from the CH_3ClN-C-OH moiety. This clearly indicates that there is no pseudoexcitation present in this TS. In effect, as in the process assisted by Ag^+, the elimination of Cl^- provokes the interchange of the nodal properties of the HOMO and LUMO of B and, consequently, the ordinary HOMO−LUMO interactions between the constituent fragments become symmetry allowed at **TSRCP**. However, these HOMO−LUMO interactions now produce a smaller stabilization of the system because the frontier MOs of the CH_3-ClN-C-OH fragment are less stable without the positive charge supplied by Ag^+ ($\epsilon_{HOMO} = -0.28$ eV, $\epsilon_{LUMO} = -0.22$ eV) and because both fragments present a lower overlap. This lower stabilization gained from the HOMO−LUMO interactions between the constituent fragments would cause the evolution of the system through C1−C2 and C1−C3 stretching and weakening of the bonding between both fragments. As a consequence of the strain energy retention and the lower

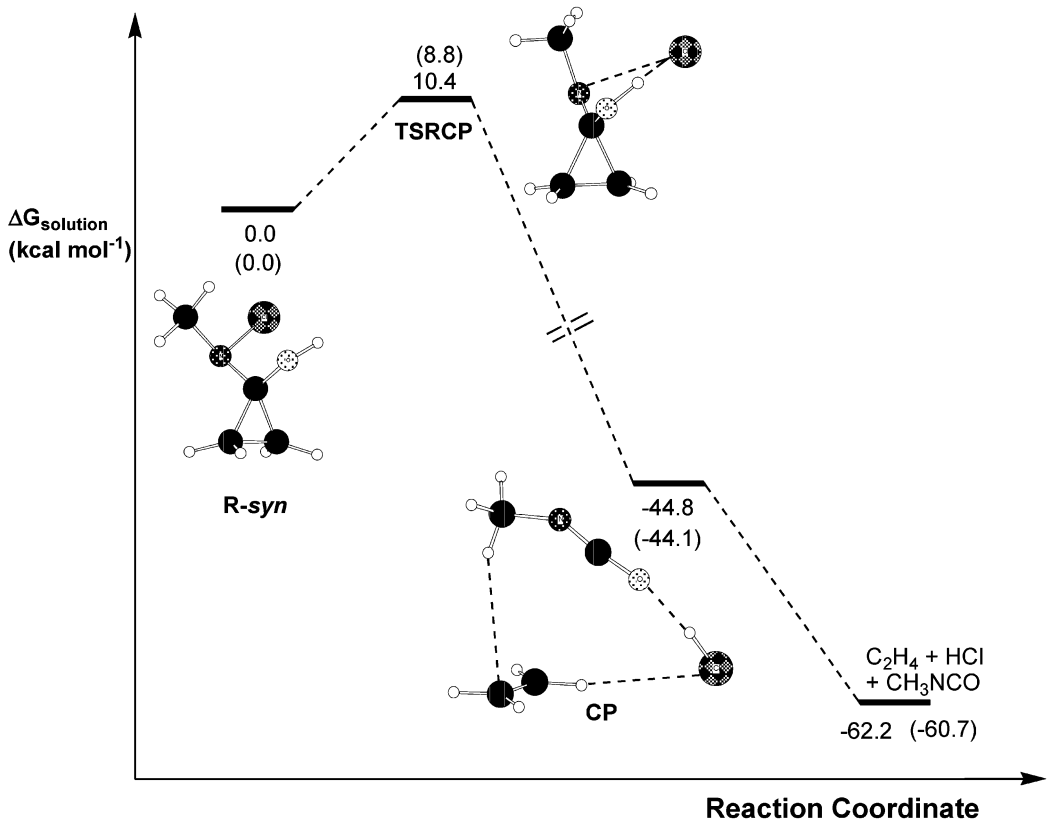

Figure 12. Gibbs energy profiles in CH_2Cl_2 (CH_3CN) solution for the elimination of Cl^- from *N*-chloro-*N*-methyl-1-hydroxycyclopropylamine without Ag^+ assistance.

TABLE 6: Relative B3LYP Electronic Energies Including the ZPVE Correction, Enthalpies, Solvation Energies, and Gibbs Energies in Gas Phase and in Solution (kcal mol^{-1}) for the Critical Structures Located along the Reaction Coordinate for the Elimination of HCl from *N*-Chloro-*N*-methyl-1-hydroxycyclopropylamine without Ag^+ Assistance

structure	$\Delta(E_{elec} + ZPVE)$	ΔH	ΔG_{gas}	$\Delta\Delta G_{solvation}$ CH_2Cl_2/CH_3CN	$\Delta G_{solution}$ CH_2Cl_2/CH_3CN
R-syn	0.0	0.0	0.0	0.0/0.0	0.0/0.0
TSRCP	20.2	20.3	19.9	−9.5/−11.1	10.4/8.8
CP	−38.8	−35.4	−48.1	3.3/4.0	−44.8/−44.1
P[a]	−35.6	−32.9	−57.7	−4.5/−2.9	−62.2/−60.7

[a] **P** = HCl + C_2H_4 + *N*-methylisocianate.

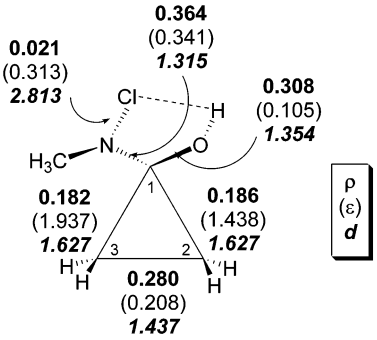

Figure 13. Most important bond lengths (Å) for **TSRCP** and the corresponding electron density, ρ, (au) and ellipticity, ϵ, evaluated at the bond critical points.

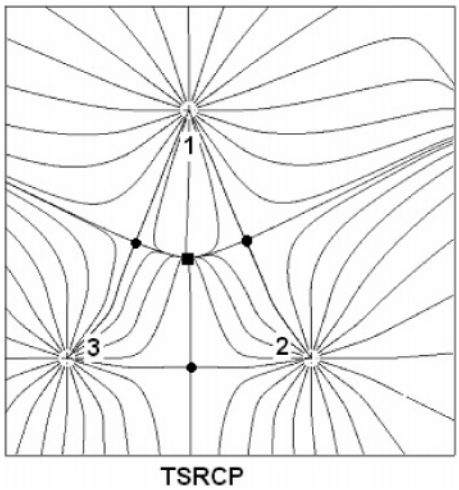

Figure 14. Map of the gradient vector field of the electronic charge density of **TSRCP** in the plane containing the nuclei of the ring. Bond critical points are denoted by solid circles, and the ring critical point is denoted by a solid square.

stabilization from the HOMO−LUMO interactions, **TSRCP** presents a larger electronic energy barrier than **TSCAGI**.

The NBO analysis renders I in Figure 16 as the most important Lewis structure of **TSRCP**. Now the interaction of the HOMO of the ethylene moiety with the LUMO of the CH_3-ClN-C-OH fragment determines a two-electron three-center interaction involving N, C1, and C2 while the Cl^- is separated from the rest of the system. Another important Lewis structure is II in Figure 16, which presents the system divided into Cl^-, CH_3N-C-OH, and C_2H_4. From this structure it is easy to

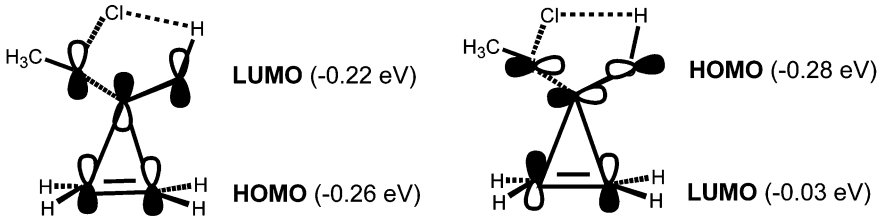

Figure 15. HOMO−LUMO interactions in the TS for Cl^- extrusion (A: C_2H_4; B: CH_3ClN-C-OH).

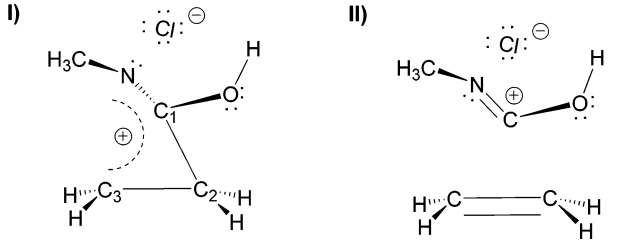

Figure 16. Most important Lewis structure for the TS for the extrusion of Cl^- in the absence of Ag^+.

TABLE 7: Differences between the Geometric Angles, α_c, and the Bond Path Angles, α_b, Found for the Three-Member Ring of TSRCP

angle	α_c (deg)	α_b (deg)	$\Delta\alpha = \alpha_b - \alpha_c$ (deg)
1	52.4	38.4	−14.0
2	63.8	66.7	2.9
3	63.8	63.8	0.0

TABLE 8: Coefficients and Relative Weights of the Most Important Electronic Configurations for the Transition State for Cl^- Elimination in the Absence of Ag^+ (A = C_2H_4; B = CH_3ClN-C-OH)

configuration	relative weight/coefficient
A^+B^- (HO−LU)	1.0/−0.37
AB	0.44/0.25
$A^{2+}B^{2-}$ (HO−LU/HO−LU)	0.44/0.25
$A^{\pm}B^{\mp}$ (HO−LU/HO−LU)	0.24/0.18
$A^{\pm}B^{\mp}$ (HO−LU/4NHO−LU)	0.24/0.18

understand that the system will evolve from **TSRCP** through Cl^- carrying the hydroxyl hydrogen atom and leaving a lone pair of electrons on the O atom, which will form a π system with C1 orthogonal to the C−N one, thus determining the fragmentation of the system in ethylene, HCl, and *N*-methylisocianate. Therefore, this analysis shows that the elimination of chloride from *N*-chloro-*N*-methyl-1-hydroxycyclopropylamine without the assistance of Ag^+ causes the weakening of the bonding between the C_2H_4 and the CH_3ClN-C-OH fragments and, ultimately, the fragmentation of the system in HCl, CH_3N-C-O, and C_2H_4 when the leaving Cl^- carries the hydroxyl hydrogen atom.[38]

In summary, in the silver-induced ring expansion of *N*-chloro-*N*-methyl-1-hydroxycyclopropylamine to form *N*-methyl-2-azetidinone, the partial Ag^+-assisted extrusion of Cl^- at the rate-determining TS provokes an important change in the nodal properties of the frontier MOs of the $CH_3ClNCOHAg^+$ fragment, thus making very stabilizing HOMO−LUMO interactions between this fragment and the C_2H_4 moiety possible. This interaction leads to the ring opening and the release of most of the strain energy, giving rise to an important reduction of the energy barrier for the process. Further, Ag^+ prevents the leaving Cl^- from carrying the hydroxyl hydrogen atom, which would give rise to the formation of HCl, CH_3N-C-O, and C_2H_4. Therefore, the Ag^+ assistance consists not simply in favoring the process by reducing an energy barrier, but it plays a crucial role in avoiding the fragmentation of the system thus making the formation of a β-lactam possible.

Acknowledgment. We thank Principado de Asturias for financial support (PB02-45 FICyT).

Supporting Information Available: Optimized structures, absolute electronic energies, and ZPVE corrections of all of the critical structures located in this work. This material is available free of charge via the Internet at http://pubs.acs.org.

References and Notes

(1) Dürckheimer, W.; Blumbach, J.; Lattrell, R.; Scheunemann, K. H. *Angew. Chem., Int. Ed. Engl.* **1985**, *24*, 180.

(2) Hart, D. H.; Ha, D. C. *Chem. Rev.* **1989**, *89*, 1447.

(3) Backes, I. *Organische Stickstoffverbindungen II: Methoden Der Organischen Chemie (Houben-Weyl)*; Georg Thieme Verlag: Stuttgart, Germany, 1991.

(4) *The Chemistry of β-Lactams*; Page, M. I., Ed.; Chapman and Hall: New York, 1992.

(5) *Organic Chemistry of β-Lactams*; Georg, G. I., Ed.; VCH: New York, 1993.

(6) De Kimpe, N. In *Comprehensive Heterocyclic Chemistry II*; Padwa, A., Ed.; Elsevier: Oxford, U.K., 1996; Vol. 1.

(7) Moore, H. W.; Goldish, D. M. In *The Chemistry of Halides, Pseudo-Halides and Azides (Supplement D)*; Patai, S., Rappoport, Z., Eds.; John Wiley and Sons: New York, 1983.

(8) Carroll, R. D.; Reed, L. L. *Tetrahedron Lett.* **1975**, 3435.

(9) Skiles, J. W.; McNel, D. *Tetrahedron Lett.* **1990**, *31*, 7277.

(10) Wasserman, H. H.; Cochoy, R. E.; Baird, M. S. *J. Am. Chem. Soc.* **1969**, *91*, 2375.

(11) Wasserman, H. H.; Adickes, H. W.; de Ochoa, O. E. *J. Am. Chem. Soc.* **1971**, *93*, 5586.

(12) Wasserman, H. H. *Angew. Chem., Int. Ed. Engl.* **1972**, *4*, 332.

(13) Wasserman, H. H.; Glazer, E. A.; Hearn, M. J. *Tetrahedron Lett.* **1973**, 4855.

(14) Wasserman, H. H.; Glazer, E. A. *J. Org. Chem.* **1975**, *40*, 1505.

(15) (a) Wasserman, H. H.; Hlasta, D. J.; Tremper, A. W.; Wu, J. S. *J. Org. Chem.* **1981**, *46*, 2999. (b) Wasserman, H. H.; Hlasta, D. J. *J. Am. Chem. Soc.* **1978**, *100*, 6780.

(16) De Kimpe, N.; Tehrani, K. A.; Fonck, G. *J. Org. Chem.* **1996**, *61*, 6500.

(17) Campomanes, P.; Menéndez, M. I.; Sordo, T. L. *J. Org. Chem.* **2003**, *68*, 6685.

(18) Frisch, M. J.; Trucks, G. W.; Schlegel, H. B.; Scuseria, G. E.; Robb, M. A.; Cheeseman, J. R.; Zakrzewski, V. G.; Montgomery, J. A., Jr.; Stratmann, R. E.; Burant, J. C.; Dapprich, S.; Millam, J. M.; Daniels, A. D.; Kudin, K. N.; Strain, M. C.; Farkas, O.; Tomasi, J.; Barone, V.; Cossi, M.; Cammi, R.; Mennucci, B.; Pomelli, C.; Adamo, C.; Clifford, S.; Ochterski, J.; Petersson, G. A.; Ayala, P. Y.; Cui, Q.; Morokuma, K.; Malick, D. K.; Rabuck, A. D.; Raghavachari, K.; Foresman, J. B.; Cioslowski, J.; Ortiz, J. V.; Stefanov, B. B.; Liu, G.; Liashenko, A.; Piskorz, P.; Komaromi, I.; Gomperts, R.; Martin, R. L.; Fox, D. J.; Keith, T.; Al-Laham, M. A.; Peng, C. Y.; Nanayakkara, A.; Gonzalez, C.; Challacombe, M.; Gill, P. M. W.; Johnson, B. G.; Chen, W.; Wong, M. W.; Andres, J. L.; Head-Gordon, M.; Replogle, E. S.; Pople, J. A. *Gaussian 98*, revision A.6; Gaussian, Inc.: Pittsburgh, PA, 1998.

(19) (a) Becke, D. *Phys. Rev. A* **1988**, *38*, 3098. (b) Lee, C.; Yang, W.; Parr, R. G. *Phys. Rev. B* **1988**, *37*, 785. (c) Becke, A. D. *J. Chem. Phys.* **1993**, *98*, 5648.

(20) Hehre, W. J.; Radom, L.; Pople, J. A.; Schleyer, P. v. R. *Ab Initio Molecular Orbital Theory*; Wiley: New York, 1986.

(21) Hay, P. J.; Wadt, W. R. *J. Chem. Phys.* **1985**, *82*, 270.

(22) Schlegel, H. B. *J. Comput. Chem.* **1982**, *3*, 214.

(23) (a) Gonzalez, C.; Schlegel, H. B. *J. Chem. Phys.* **1989**, *90*, 2154. (b) Gonzalez, C.; Schlegel, H. B. *J. Phys. Chem.* **1990**, *84*, 5523.

(24) McQuarrie, D. A. *Statistical Mechanics*; Harper & Row: New York, 1976.

(25) Rivail, J. L.; Rinaldi, D.; Ruiz-López, M. F. In *Theoretical and Computational Model for Organic Chemistry*, *NATO ASI Series C*; Formosinho, S. J., Csizmadia, I. G., Arnaut, L., Eds.; Kluwer Academic Publishers: Dordrecht, The Netherlands, 1991; Vol. 339.

(26) Tomasi, J.; Persico, M. *Chem. Rev.* **1994**, *94*, 2027.

(27) (a) Cramer, C. J.; Truhlar, D. G. In *Reviews in Computational Chemistry*; Lipkowitz, K. B., Boyd, D. B., Eds.; VCH: New York, 1995; Vol. 6. (b) Rivail, J. L.; Rinaldi, D. In *Computational Chemistry: Review of Current Trends*; Leszczynski, J., Ed.; World Scientific: New York, 1995. (c) Cramer, C. J.; Truhlar, D. G. *Chem. Rev.* **1999**, *99*, 2161.

(28) Claverie, P. In *Quantum Theory of Chemical Reactions*; Daudel, R., Pullman, A., Salem, L., Veillard, A., Eds.; Reidel: Dordrecht, The Netherlands, 1982; Vol. 3.

(29) (a) Miertus, S.; Scrocco, E.; Tomasi, J. *Chem. Phys.* **1981**, *55*, 117. (b) Cammi, R.; Tomasi, J. *J. Comput. Chem.* **1995**, *16*, 1449. (c) Cossi, M.; Barone, V.; Cammi, R.; Tomasi, J. *Chem. Phys. Lett.* **1996**, *255*, 327. (d) Barone, V.; Cossi, M.; Tomasi, J. *J. Chem. Phys.* **1997**, *107*, 3210. (e) Amovilli, C.; Barone, V.; Cammi, R.; Cancès, E.; Cossi, M.; Menucci, B.; Pomelli, C. S.; Tomasi, J. *Adv. Quantum. Chem.* **1998**, *32*, 227.

(30) (a) Bader, R. F. W. *Atoms in Molecules. A Quantum Theory*; Oxford University Press: Oxford, U.K., 1990. (b) Bader, R. F. W.; Popelier, P. L. A.; Keith, T. A. *Angew. Chem., Int. Ed. Engl.* **1994**, *33*, 620.

(31) Biegler-Konig, F. W.; Bader, R. F. W.; Hua-Tang, T. *J. Comput. Chem.* **1982**, *3*, 317.

(32) Fujimoto, H.; Kato, S.; Yamabe, S.; Fukui, K. *J. Chem. Phys.* **1974**, *60*, 572.

(33) López, R.; Menéndez, M. I.; Suárez, D.; Sordo, T. L.; Sordo, J. A. *Comput. Phys. Commun.* **1993**, *76*, 235.

(34) (a) Reed, E.; Curtiss, L. A.; Weinhold, F. *Chem. Rev.* **1988**, *88*, 899. (b) Weinhold, F.; Carpenter, J. E. In *The Structure of Small Molecules and Ions*; Naaman, R., Vager, Z., Eds.; Plenum Press: New York, 1988.

(35) Diaz, N.; Suárez, D.; Sordo, T. L. *Chem.—Eur. J.* **1999**, *5*, 1045.

(36) (a) Wiberg, K. W. *Angew. Chem., Int. Ed. Engl.* **1986**, *25*, 312. (b) Wiberg, K. W.; Fenoglio, R. A. *J. Am. Chem. Soc.* **1968**, *25*, 312.

(37) (a) Inagaki, S.; Fujimoto, H.; Fukui, K. *J. Am. Chem. Soc.* **1975**, *97*, 6108. (b) Fukui, K. *Theory of Orientation and Stereoselection*; Springer-Verlag: Berlin, 1975.

(38) The crucial influence of the hydroxyl hydrogen atom elimination on the fragmentation of the system is clearly reflected in the fact that when the nitrenium intermediate located along the reaction coordinate for the process assisted by Ag^+, **I**, is deprotonated its barrierless fragmentation into ethylene and *N*-methylisocianate takes place immediately.